

1 Bet-hedging antimicrobial strategies in macrophage phagosome acidification drive the dynamics of
2 *Cryptococcus neoformans* intracellular escape mechanisms

3

4 Quigly Dragotakes¹, Ella Jacobs¹, Lia Sanchez Ramirez², Insun Yoon², Caitlin Perez-Stable², Hope Eden³,
5 Jenlu Pagnotta², Raghav Vij⁴, Aviv Bergman^{5,6}, Franco D'Alessio⁷, Arturo Casadevall^{1*}

6

7 *Corresponding Author

8 ¹Department of Molecular Microbiology and Immunology, Johns Hopkins Bloomberg School of Public
9 Health, Baltimore, Maryland, USA

10 ²Department of Molecular and Cell Biology, Johns Hopkins University, Baltimore, Maryland, USA

11 ³Department of Cellular and Molecular Medicine, Johns Hopkins University School of Medicine,
12 Baltimore, Maryland, USA

13 ⁴Leibniz Institute for Natural Product Research and Infection Biology, Hans Knöll Institute

14 ⁵Department of Systems and Computational Biology, Albert Einstein College of Medicine, Bronx, NY

15 ⁶Santa Fe Institute, Santa Fe, New Mexico, USA

16 ⁷Department of Medicine, Johns Hopkins University School of Medicine, Baltimore, United States

17

18 **Abstract**

19 The fungus *Cryptococcus neoformans* is a major human pathogen with a remarkable intracellular
20 survival strategy that includes exiting macrophages through non-lytic exocytosis (Vomocytosis) and
21 transferring between macrophages (Dragotcytosis) by a mechanism that involves sequential events of
22 non-lytic exocytosis and phagocytosis. Vomocytosis and Dragotcytosis are fungal driven processes, but
23 their triggers are not understood. We hypothesized that the dynamics of Dragotcytosis could inherit the
24 stochasticity of phagolysosome acidification and that Dragotcytosis was triggered by fungal cell stress.
25 Consistent with this view, fungal cells involved in Dragotcytosis reside in phagolysosomes characterized
26 by low pH and/or high oxidative stress. Using fluorescent microscopy, qPCR, live cell video microscopy,
27 and fungal growth assays we found that the that mitigating pH or oxidative stress abrogated
28 Dragotcytosis frequency, that ROS susceptible mutants of *C. neoformans* underwent Dragotcytosis more
29 frequently. Dragotcytosis initiation was linked to phagolysosomal pH and oxidative stresses and
30 correlated with the macrophage polarization state. Dragotcytosis manifested stochastic dynamics thus
31 paralleling the dynamics of phagosomal acidification, which correlated with the inhospitality of
32 phagolysosomes in differently polarized macrophages. Hence, randomness in phagosomal acidification
33 randomly created a population of inhospitable phagosomes where fungal cell stress triggered stochastic
34 *C. neoformans* non-lytic exocytosis dynamics to escape a non-permissive intracellular macrophage
35 environment.

36

37 Introduction

38 *Cryptococcus neoformans* is a pathogenic yeast that can reside in the phagolysosome of host
39 macrophages¹. Macrophages are critical cells in the pathogenesis of cryptococcosis, being involved in
40 the containment of, and extrapulmonary dissemination of infection². Macrophages are also involved in
41 the pathogenesis of latent infection where the organism can survive for a long time in granulomas.
42 Hence, *C. neoformans* survival in macrophages is critical for both the persistence and dissemination of
43 infection. The yeasts, inhaled from the environment, manage intracellular survival by modifying the
44 phagolysosomal environment in their own favor. The capsule of *C. neoformans* is comprised of several
45 subunits including glucuronic acid and glucuronoxylomannan (GXM) which act as weak acids capable of
46 buffering the environment to pH ~5^{3,4}. *C. neoformans* also produces urease which disrupts
47 phagolysosomal acidification by breaking down urea into carbon dioxide and ammonia, a weak base⁵.
48 Additionally, *C. neoformans* are capable of exiting host macrophages through lytic exocytosis, non-lytic
49 exocytosis (Vomocytosis)⁶⁻⁸, or lateral cell-to-cell transfer (Dragotcytosis)⁹.

50

51 We recently observed that macrophages use a bet hedging strategy in phagosomal acidification to
52 maximize the antimicrobial properties of acidic pH for controlling the growth of ingested microbes¹⁰. By
53 increasing the diversity of possible phagolysosomal pH, a population of macrophages will optimize its
54 chances to inhibit pathogen growth based on pH alone. We also noticed that even small perturbations in
55 this system could disrupt the bet-hedging strategy and that different pathogens employ various
56 strategies to tip the odds in their own favor. *C. neoformans* interferes with the stochastic modulation of
57 phagosomal pH by capsule buffering and urease activity^{3,5}. Phagosomal pH varies with macrophage
58 polarization such that alternate activated M2 macrophages are less hostile¹⁰, in terms of pH, to ingested
59 *C. neoformans* yeasts.

60

61 A fascinating aspect of the interaction with *C. neoformans* with macrophages is the phenomenon of
62 fungal cell transfer between two macrophages, a process we have recently termed 'Dragotcytosis'⁹.
63 Dragotcytosis results from the coordinated exocytosis and phagocytosis events between adjacent
64 macrophages⁹. We also noted that Dragotcytosis is favorable to *C. neoformans* as macrophages with
65 Dragotcytosis blockaded yield more colony forming units after 24 h than those who were not blockaded.
66 Finally, we note that Dragotcytosis is an active process, only occurring with live *C. neoformans*⁶. When
67 taken together, these findings suggest Dragotcytosis is triggered by *C. neoformans* for a purpose
68 beneficial to the yeast. However, it is unknown what specifically triggers Dragotcytosis or how
69 transferring between macrophages confers a benefit. Notably, previous observations have established
70 that phagolysosomal pH can modulate non-lytic exocytosis frequency, supporting the idea that pH has
71 an important and complex role in the regulation of this system^{11,12}.

72

73 In addition to phagolysosomal pH there are other stressors in the phagosome that could conceivably
74 affect the rate of Dragotcytosis. The oxidative burst and the release of reactive oxygen species into the
75 phagolysosome are also potentially important. Both ROS generation and nitric oxide synthase (NOS)
76 activity are upregulated in M1 macrophages in response to phagocytosed pathogens¹³⁻¹⁵. NOS

77 metabolizes arginine into nitric oxide and citrulline. Conversely, Arginase (Arg), upregulated in M2
78 macrophages) hydrolyzes arginine to ornithine and urea. Increased activity of either Arg or NOS will
79 consume available arginine, resulting in lower efficacy of the other. Thus, M2 polarized macrophages
80 have lower NOS activity and a less significant oxidative burst, which is thought to be one of the main
81 reasons M2 macrophages are less effective at killing pathogens.

82

83 In this study, we analyzed the consequences of macrophage polarization and phagolysosomal stress on
84 *C. neoformans* pathogenesis and outcome. We hypothesized that macrophages containing *C.*
85 *neoformans* phagolysosomes that cause significant stress to the yeast by acidity and/or oxidative stress
86 would be more likely to result in Dragotcytosis events than other *C. neoformans* containing
87 phagolysosomes. In this regard, we tested whether the more fungicidal environment in M1
88 macrophages was more likely to trigger Dragotcytosis than the more permissive intracellular
89 environment of M2 macrophages. Our goal was evaluating the hypothesis that Dragotcytosis is a fungal
90 driven mechanism for escape of a hostile environment. We found that both hostile pH and reactive
91 oxygen species (ROS) in the phagolysosome drive Dragotcytosis and use modelling to show the potential
92 increasing benefit of Dragotcytosis events as a function of resident phagolysosome hostility.

93

94 **Materials and Methods**

95 *Cell Strains and Culture Conditions*

96 *Cryptococcus neoformans* species complex serotype A strain H99 was originally obtained from John
97 Perfect (Durham, NC) and *C. neoformans* H99 actin-GFP created by the May lab¹⁶. Culture stocks were
98 stored at 80 °C. Frozen stocks were later streaked onto YPD agar and incubated at 30 °C. Liquid
99 suspensions of cryptococcal cultures were grown in YPD overnight at 30 °C. Cryptococcal cultures were
100 heat killed by incubating at 65 °C for 1 h. Mutant strains were obtained from a previously published
101 knockout library¹⁷.

102

103 Bone marrow derived macrophages (BMDMs) were harvested from 6 week old C57BL/6 female mice
104 from The Jackson Laboratory from hind leg bones and were differentiated by seeding in 10 cm tissue
105 culture treated dishes in DMEM with 10% FBS, 1% nonessential amino acids, 1% penicillin-streptomycin,
106 2 mM Glutamax, 1% HEPES buffer, 20% L-929 cell conditioned supernatant, 0.1% beta-mercaptoethanol
107 for 6 days at 37 °C and 9.5% CO₂. BMDMs were used for experiments within 5 days after differentiation.
108 BMDMs were activated with 0.5 ug/mL LPS and 10 ng/mL IFN- γ for M1 polarization or 20 ng/mL IL-4 for
109 M2 polarization for 16 h prior to experiments.

110

111 *Phagolysosomal pH measurement*

112 Phagolysosomal pH was measured using ratiometric fluorescence imaging involving the use of pH-
113 sensitive probe Oregon green 488 as described in prior studies⁵. Briefly, Oregon green 488 was first

114 conjugated to mAb 18B7 using Oregon Green 488 Protein Labeling Kit (ThermoFisher). BMDMs were
115 plated at a density of 1.25×10^5 cells/well on 24-well plate with 12 mm circular coverslip. Cells were
116 activated with 0.5 $\mu\text{g}/\text{ml}$ LPS and 100 U/ml IFN- γ or 20 ng/ml IL-4 as previously described at 37 °C in a
117 9.5% CO₂ atmosphere overnight. Prior to infection, 2 d old live H99, heat killed H99, or anti-mouse IgG
118 coated polystyrene bead (3.75×10^6 cells or beads/ml) were incubated with 10 $\mu\text{g}/\text{ml}$ Oregon green
119 conjugated mAb 18B7 for 15 min. Macrophages were then incubated with Oregon green conjugated
120 mAb 18B7-opsionized particles in 3.75×10^5 cryptococcal cells or beads per well. Cells were either
121 centrifuged immediately at 350 x g for 1 min and incubated at 37 °C for 10 min or incubated at 4 °C for
122 30 min to synchronize ingestion and allow phagocytosis. Extracellular cryptococcal cells or beads were
123 removed by washing three times with fresh medium, a step that prevents the occurrence of new
124 phagocytic events. As an additional safeguard against new phagocytic events fresh media was
125 supplemented with AlexaFluor 568 conjugated mAb 18B7 for 1 h to label extracellular particles. Samples
126 were collected at their respective time points after phagocytosis by washing the coverslip twice with
127 pre-warmed HBSS and placing it upside down on a MatTek petri dish (35 mm with 10 mm embedded
128 coverslip well) with HBSS in the microwell. Images were taken by using Olympus AX70 microscopy with
129 objective 40x at dual excitation 440 nm and 488 nm, and emission 520 nm. Images were analyzed using
130 MetaFluor Fluorescence Ratio Imaging Software. Fluorescence intensities were used to determine the
131 ratios of Ex488 nm/Ex440 nm that were converted to absolute pH values using a standard curve where
132 the images are taken as above but intracellular pH of macrophages was equilibrated by adding 10 μM
133 nigericin in pH buffer (140 mM KCl, 1 mM MgCl₂, 1 mM CaCl₂, 5 mM glucose, and appropriate buffer \leq
134 pH 5.0: acetate-acetic acid; pH 5.5-6.5: MES; \geq pH 7.0: HEPES. Desired pH values were adjusted using
135 either 1 M KOH or 1 M HCl). The pH of buffers was adjusted at 3-7 using 0.5-pH unit increments.

136

137 *Cryptococcal Capsule Measurements*

138 Capsule measurements were acquired by measuring exclusion zones on India Ink slides and phase
139 contrast microscopy. To determine differences between polarized macrophage incubations, *C.*
140 *neoformans* were harvested after being ingested by macrophages for 24 h. Extracellular yeasts were first
141 removed by washing the cells 3 times with 1 mL HBSS. Macrophages were lifted from their plates,
142 centrifuged at 350 x g for 10 min, and resuspended in 1 mL distilled H₂O. Cells were then passed through
143 a 27 $\frac{3}{4}$ gauge needle 10 times and left incubating for 20 total min to ensure lysis. After lysis *C.*
144 *neoformans* were pelleted via centrifugation at 2300 x g for 5 min and resuspended in 50 μL of PBS.
145 Slides were prepared using 8 μL of cell mixture and 1.5 μL India ink, then imaged on an Olympus AX70 at
146 20x objective. Capsules and cell bodies were measured using a previously published measuring
147 program¹⁸.

148

149 *NOS and Arginase Activity Measurements*

150 BMDMs were seeded at 10^6 cell/well in 6-well treated tissue culture plates and activated overnight for
151 M0, M1, or M2 polarization as previously described. Prior to infection, 2 d old live H99 (10^6 cells/well)
152 were incubated with 10 $\mu\text{g}/\text{ml}$ mAb 18B7 for 10 min. Macrophages were then incubated with opsonized

153 particles at MOI 1. Cells were either centrifuged immediately at 350 x *g* for 1 min or incubated at 4 °C for
154 30 min to synchronize ingestion and cultures were incubated at 37 °C for 10 min to allow phagocytosis.
155 Extracellular cryptococcal cells were removed by washing three times with fresh medium, a step that
156 prevents the occurrence of new phagocytic events. After 24 hours, cell supernatant was collected and
157 the BMDMs were lysed with distilled water and 10 passages through a syringe with 23G needle. The
158 supernatant was tested for NO levels via Greiss reagent kit (Millipore-Sigma G4410). Cell lysates were
159 tested for arginase activity with arginase activity assay kit (Millipore-Sigma MAK112).

160

161 *Cryptococcus neoformans* Viability and Growth Inhibition

162 BMDMs were seeded (10⁶ cells/well) in 6-well tissue culture plates. The cells were activated overnight
163 (16 h) with IFN γ (0.02 μ g/mL) and (0.5 μ g) LPS for M1, IL-4 (20 ng/mL) for M2, or unstimulated for M0.
164 The cells were then infected with a 2 d culture of *C. neoformans* opsonized with 18B7 (10 μ g/mL) at an
165 MOI of 1 for 2 or 24 h. At the respective timepoint, the supernatant was collected and total yeast cells as
166 well as GFP positive yeast were counted by hemocytometer and fluorescence microscopy using an
167 Olympus AX70. *C. neoformans* ingested by adherent macrophages were imaged on a Zeiss Axiovert
168 200M inverted scope in a live cell incubator chamber. Viability was calculated as the proportion of yeast
169 cells expressing GFP-actin.

170

171 The collected, conditioned supernatant was then pelleted at 2300 x *g* for 5 min to remove debris and
172 extracellular crypto. Supernatants were seeded with 5 x 10⁴ cell / mL of *C. neoformans* and absorbance
173 (600 nm) as well as fluorescence (GFP 488/510) was read at 0 and 24 h. Samples were prepared on glass
174 slides with India Ink negative stain and imaged with an Olympus AX70. Growth was characterized by
175 increase in OD600 and viability was measured as the proportion of GFP positive cells.

176

177 *Dragotcytosis Frequency Measurements*

178 BMDMs were seeded (5 x 10⁴ cells/well) in MatTek dishes. The cells were activated overnight (16 h) with
179 IFN γ (0.02 μ g/mL) and (0.5 μ g) LPS for M1, IL-4 (20 ng/mL) for M2, or unstimulated for M0. Cells in the
180 MatTek dish were infected with Uvitex 2B (5 μ m/mL) stained and 18B7 (10 μ g/mL) opsonized *C.*
181 *neoformans* at an MOI of 3 for 1 h, then supplemented with 2 mL fresh media and 18B7 mAb. In the
182 case of drug trials this fresh media was also supplemented with bafilomycin A1 (100 nM), chloroquine (6
183 μ m), fluconazole (20 μ g / μ L), or amphotericin B (0.5 μ g / μ L). MatTek dishes were then placed under a
184 Zeiss axiovert 200M 10X magnification, incubated at 37 °C or 30 °C and 9.5% CO₂, and imaged every 2
185 min for a 24 h period. Images were then manually analyzed to identify ingested yeast cell outcomes.

186

187 *Modelling*

188 To simulate the effect of Dragotcytosis on a population of *C. neoformans* in phagolysosomes we
189 generated 10,000 hypothetical phagolysosomal pH values based on the distribution of observed

190 phagolysosomal pH in M1 polarized bead containing macrophage phagolysosomes. Each value < 4 was
191 replaced one time by randomly determining a new phagolysosomal pH from the same distribution to
192 simulate a Dragocytosis event from the initial macrophage to a random new one.

193

194 *Data Analysis for Stochastic Signatures*

195 Discrimination of deterministic vs. stochastic dynamics was achieved using the previously characterized
196 permutation spectrum test¹⁹ and the methods outlined in our previous work¹⁰. In short, processed
197 datasets are aligned in a vector and separated into subgroups by a scanning window of 4 units. Each of
198 the overlapping four-unit segments are then assigned a value from 0 to 3 based on their relative size
199 (the largest value being 3 and the least being 0) in what is referred to as an ordinal pattern. The
200 frequencies for each pattern are calculated for the entire dataset. Determinism is characterized by
201 observations of ordinal patterns that do not exist (forbidden patterns), whereas stochastic dynamics are
202 characterized by every ordinal pattern existing at a non-zero frequency. In this work, the original data is
203 the time interval between the initiation of each instance of host cell escape within an experiment.

204

205 *qPCR*

206 BMDMs were seeded at 10^6 cell/well in 6-well treated tissue culture plates and activated overnight for
207 M0, M1, or M2 polarization as previously described. Prior to infection, 2 d old live H99 or inert beads
208 (10^6 particles/well) were incubated with 10 μ g/ml mAb 18B7 for 10 min. Macrophages were then
209 incubated with opsonized particles at MOI 1. Cells were either centrifuged immediately at 350 x g for 1
210 min or incubated at 4 °C for 30 min to synchronize ingestion and cultures were incubated at 37 °C for 10
211 min to allow phagocytosis. Extracellular cryptococcal cells were removed by washing three times with
212 fresh medium, a step that prevents the occurrence of new phagocytic events. After 24 hours, BMDMs
213 were resuspended in TRIzol reagent and frozen at -80°C. Total RNA was isolated from frozen cell cultures
214 using the TRIzol reagent per the manufacturer's suggestions (Invitrogen, Carlsbad, CA). The RNA was
215 precipitated in isopropanol and then subjected to additional purification using the RNeasy RNA isolation
216 kit (Qiagen, Valencia, CA) according to the manufacturer's instructions. RNA was reverse transcribed to
217 generate cDNA using a First-Strand Synthesis kit (Amersham) and random hexamers as primers. The
218 cDNA was then used as the template for quantitative PCR using an iCycler Thermal Cycler Real-Time PCR
219 machine (Bio-Rad, Hercules, CA). The products of PCR amplification were detected with Syber green
220 fluorescent dye and the relative expression of each gene of interest expressed with reference to that of
221 glyceraldehyde phosphate dehydrogenase (GAPDH). The PCR products were analyzed on Tris-Acetate-
222 EDTA agarose gels to confirm its correct size.

223

224 *Macrophage Preference Assay*

225 To ascertain whether *C. neoformans* preferred residence in macrophages as a function of host cell
226 polarization we carried out cell transfer experiments in macrophage populations consisting of mixed M0,
227 M1, and M2 polarized cells. BMDMs were seeded at 3×10^4 cells per well in a 24 well tissue culture plate
228 loaded with circular coverslips then activated overnight for M1 polarization as previously described.

229 Three separate populations of BMDMs were seeded in dishes large enough to account for an additional
230 3×10^4 cells per well per condition and activated overnight for M0, M1, or M2 polarization as previously
231 described. The initial population of M1 BMDMs on coverslips was infected with 6×10^4 18B7 opsonized
232 *C. neoformans* yeasts per well for 1 h. The remaining three populations of uninfected BMDMs were
233 stained with CellTracker CMFDA (Green). After the 1 h infection the three labeled populations of
234 BMDMs were lifted with cellstripper and added to the unlabeled, infected M1 coverslips so that each
235 coverslip had two populations of macrophages: 1. Unlabeled and infected M1 and 2. Labeled but
236 uninfected M0, M1, or M2. The coverslips were then incubated for 24 h at 37 °C and 9.5% CO₂ for 24, 48,
237 or 72 h. The cells were then fixed with 4% paraformaldehyde for 10 min at room temperature and
238 coverslips were mounted on slides with ProLong Gold Antifade Mountant (Thermofisher) and imaged on
239 an Olympus AX70. For each field of view the total number of each macrophage population was counted
240 along with how many infected macrophages in each population. To correct for floating cells and ensure
241 a proper count of total cells, a hemocytometer was used to enumerate the total number of floating cells
242 in each sample. We assumed any floating cells were previously evenly distributed across the original
243 sample and thus used the percent of floating cells to estimate the number of missing cells in any given
244 sample using the formula below:

$$T'_G = \left[\frac{T_G}{1 - \frac{SN_G}{I_G}} \right]$$

245 T_G = Total green positive cells counted on a given field of view

246 SN_G = Total number of green cells in supernatant per hemocytometer

247 I_G = Total amount of green cells plated initially

248

249 *Modeling Dragotcytosis Dynamics*

250 A population of 40,000 cells was generated consisting of 10,000 cells each of infected M1, uninfected
251 M1, uninfected M2, and uninfected M0 macrophages. During each iteration of Dragotcytosis each
252 infected cell had a random chance of experiencing Dragotcytosis or Vomocytosis based on observed
253 frequencies *in vitro*. A Vomocytosed yeast was considered removed from the modeling experiment as
254 we did not have an accurate way to model reuptake, and a Dragotcytosed yeast was randomly
255 transferred to one of the four types of macrophage cells with no bias introduced. 10 rounds of
256 sequential Dragotcytosis were modeled and the entire experiment was replicated 100 times.

257

258 *Statistical analysis*

259 Specific statistical tests for each experiment are denoted in the figure legends with tests for multiple
260 hypotheses. When comparing frequency of host cell exit strategies, we compared mutant strains to the
261 wild-type strain with a test of equal proportions and Bonferroni multiple hypothesis correction.

262

263 Results

264

265 *Macrophage Polarization State Affects Frequency of Host Escape Events*

266 Given our prior findings showing different acidification dynamics in differently polarized macrophages¹⁰,
267 we investigated whether macrophage polarization effected the frequency of Dragotcytosis. First, to
268 ensure that our results were not confounded by differing population densities of macrophages resulting
269 in higher or lower frequencies of events, we compared Dragotcytosis frequency to macrophage density
270 and found no correlation (**Supplemental Figure 1**). Analysis of the pH distribution in cryptococcal
271 phagosomes, M2 macrophages are more hospitable than M1 macrophages *C. neoformans*, having a
272 higher proportion of macrophages at optimal growth pH (~5.5) and few phagolysosomes at inhibitory
273 ranges (≤ 4) (**Figure 1A**). Using M0 macrophages as a baseline measure of Dragotcytosis frequency, we
274 find that M1 polarization increases Dragotcytosis frequency while M2 polarization completely abrogates
275 Dragotcytosis. (**Figure 2, Supplemental Figure 2**). This result correlates the frequency of Dragotcytosis
276 with the relative hospitality of each type of macrophage phagolysosome. When taken in context with
277 the previously reported insight that Dragotcytosis is an active process which is beneficial for *C.*
278 *neoformans* survival⁹, these data suggest that Dragotcytosis is more likely to be initiated in hostile
279 phagolysosomes.

280

281 *Cryptococcus neoformans* Capsule and Cell Body Size are Unaffected by Polarization

282 The *C. neoformans* capsule is one of the most important virulence factors and determinants of infection
283 outcome and a powerful modulator of phagolysosomal pH³. Capsule growth could modulate
284 phagolysosomal pH by mechanically stressing the phagolysosomal membrane as it enlarges, causing the
285 phagolysosome to become leaky²⁰. Several aspects of cryptococcal pathology and phagolysosomal
286 outcome are correlated to capsule size including buffering potential^{3,20}. To investigate whether the
287 changes in pH in differently polarized macrophages were due to capsule differences, we measured
288 capsule sizes after infection of differently polarized macrophages. We found that the average and
289 median capsule sizes did not appreciably differ between populations of *C. neoformans* ingested by
290 differently polarized macrophages, nor did the average and median cell body sizes (Supplemental Figure
291 3). Furthermore, if phagolysosomal pH was modulated by capsule size, we would expect to observe a
292 correlation between cell radius and phagolysosomal pH. We found no indication of a correlation
293 between particle size and phagolysosomal pH, even if we began measuring clusters of multiple particles
294 within a single phagolysosome (**Supplemental Figure 4**).

295

296 *Macrophage Polarization Modulates Oxidative Response and Affects C. neoformans* Viability

297 To determine whether the macrophage oxidative response varied between polarization states in a
298 manner that would support our hypothesis on the triggers of Dragotcytosis frequency, we measured
299 NOS and Arg1 activity between macrophage populations. M2 macrophages had the lowest NOS activity
300 and the highest Arg1 activity, while M1 macrophages had the highest NOS activity with the lowest Arg1
301 activity. (**Figure 1B and C**). This data supports the notion that M2 macrophage phagolysosomes are more

302 hospitable for *C. neoformans*. Additionally, by comparing enzymatic activity between macrophages
303 infected or uninfected with *C. neoformans* we found that infection lowers NOS activity in M0 and M2
304 populations while increasing Arg1 activity in M1 populations (**Figure 1B** and C). Each of these changes
305 would result in more hospitable phagolysosomes for *C. neoformans*.

306

307 We used GFP expression behind an actin promoter as a surrogate for viability for internalized *C.*
308 *neoformans* in macrophages. Whether or not GFP negative cells are truly “dead” is a philosophical
309 question beyond the scope of this paper, but a cell that does not express actin would certainly be
310 incapable of division. Thus, we explored viability in terms of fungistatic rather than fungicidal qualities.
311 We found that, at two hours post infection, *C. neoformans* ingested by M1 or M0 macrophages were
312 less viable than those in M2 macrophages (**Figure 1D**). Additionally, we investigated the viability of
313 extracellular *C. neoformans* and found that at 24 h post infection extracellular yeasts cultured with M1
314 macrophages are still inhibited (**Figure 1E** and F). This is consistent with prior reports that macrophages
315 can inhibit extracellular *C. neoformans* cells^{21,22}. We hypothesize this inhibition is due to the buildup of
316 NO in the extracellular media. We found no extracellular crypto at 2 hours post infection consistent with
317 our observations that exocytosis occurs hours after ingestion.

318

319 Finally, to investigate whether *C. neoformans* infection modulates macrophage polarization during
320 infection, we performed qPCR on RNA harvested from differently polarized macrophages 24 h after
321 infection. We found that *C. neoformans* infection alone, in M0 macrophages, skews toward M2
322 polarization (**Figure 1G**). This effect is augmented in M2 macrophages activated beforehand with IL-4
323 suggesting that *C. neoformans* may actively skew macrophages toward the most hospitable state. We
324 did not see such synergism when macrophages were stimulated with IFN γ and LPS, or when
325 macrophages were not stimulated.

326

327 *Phagolysosome pH is Associated with Dragotcytosis Frequency*

328 To probe whether phagosomal pH modulated Dragotcytosis frequency rather than other downstream
329 effects of polarization, we altered phagosomal pH in M1 macrophages with various drugs. Chloroquine is
330 a weak base that localizes to phagolysosomes and can be used to alkalinize macrophage phagolysosomes
331 *in vitro*, and at 6 μ M buffers phagolysosomes to a pH optimal *C. neoformans* growth. Bafilomycin A1 is a
332 V-ATPase inhibitor which prevents protons from being pumped into the organelle. Alkalinization of M1
333 cryptococcal phagosomes with either drug abrogated Dragotcytosis (**Figure 2**), consistent with the
334 notion that phagosomal acidification triggers lateral cell transfer. Interestingly, treatment with sub-
335 inhibitory concentrations of Fluconazole (20 μ g / μ L) and Amphotericin B (0.5 μ g / μ L) also reduced the
336 frequency of Dragotcytosis.

337

338 *Disrupting Macrophage Anti-Fungal Function Lowers Dragotcytosis Frequency*

339 If Dragotcytosis is triggered by fungal cell stress, then further disrupting the macrophages' ability to
340 inhibit *C. neoformans* would be expected to lower its overall frequency. We investigated this using two

341 methodologies. First, we infected macrophages with *C. neoformans* induced to grow large capsules. The
342 sheer size of cell as well as the anti-phagocytic properties of the capsule are known to inhibit
343 macrophage uptake and promote fungal survival. We found that capsule induced *C. neoformans*
344 Dragotcytosed less frequently and Vomocytosed dramatically more often compared to wild-type,
345 resulting in no overall change when comparing both types of events together (**Figure 2A**). Next, we
346 infected macrophages with wild-type *C. neoformans* at 30 °C, a temperature optimal for the fungus and
347 suboptimal for the macrophage. We again found that Dragotcytosis was abrogated (**Figure 2A**). Taken
348 together these results support the hypothesis that Dragotcytosis is induced when *C. neoformans* are
349 stressed or overwhelmed by host macrophage defenses. Finally, we investigated whether melanized *C.*
350 *neoformans* Dragotcytosed at different frequencies as melanin is known to protect from
351 phagolysosomal stressors²³⁻²⁵. We found that melanized yeast underwent Dragotcytosis at a reduced
352 rate (**Figure 2A**). This especially raised the possibility that Dragotcytosis could be triggered by general
353 cellular stress within the phagolysosome rather than pH specifically.

354

355 *Oxidative Stress Modulates Dragotcytosis Frequency*

356 To further probe whether oxidative stress had a role in triggering host cell escape, we investigated
357 several mutant *C. neoformans* strains deficient in various oxidative stress mitigation pathways including:
358 Superoxide Dismutases 1 and 2 (SOD1, SOD2), Catalases 1 and 3 (Cat1, Cat3), Thiorexodin 1 (TXN), and
359 Glutathione Peroxidases 1 and 2 (GPx and GPx2)¹⁷. Δ SOD1, Δ Cat1, Δ Cat3, Δ TXN, Δ GPx, and Δ GPx2 strains
360 of *C. neoformans* underwent Dragotcytosis at an increased frequency compared to the wild-type
361 parental strain KN99, while Dragotcytosis frequency in Δ SOD2 and Δ TXN2 remained unchanged (**Figure**
362 **2B**). Overall, these data support the notion that Dragotcytosis is triggered by a stressed yeast, and that
363 increasing stress on the yeast results in increased Dragotcytosis.

364

365 *Time to Host Exit Initiation is Stochastic for Exocytosis Events*

366 If Vomocytosis and/or Dragotcytosis are triggered by hostile pH and final pH is determined stochastically
367 from a normal distribution¹⁰, then these host cell exocytosis events should also display stochastic
368 dynamics resembling those of the upstream pH trigger. To explore whether the stochasticity of
369 phagolysosome acidification is preserved in this system, we measured the time at which each process
370 occurs throughout a series of videos of macrophages infected with *C. neoformans*. We found that while
371 the time of exocytosis events was not normally distributed, these events were triggered stochastically
372 with no forbidden ordinal patterns observed (**Figure 3A** and B). The absence of forbidden ordinals
373 implies that the process is not deterministic, ruling out chaotic dynamics.

374

375 *Simulation Data Suggests Dragotcytosis at low pH Benefits Cryptococcal Cells*

376 We hypothesized that triggering Dragotcytosis, or non-lytic exocytosis, in phagolysosomes of low pH
377 would benefit *C. neoformans* cells by lowering the total number of yeasts within inhibitory
378 phagolysosomes. The argument for non-lytic exocytosis is intuitive, in that the yeast leaves the
379 phagolysosome altogether and could only result in fewer inhibitory phagolysosomes. Dragotcytosis

380 however is more nuanced as there is no obvious way for *C. neoformans* to know whether the new
381 phagolysosome will be more or less hostile to the yeast. To explore this hypothesis, we modeled
382 phagolysosomal pH distributions based on observed pH measurements of bead containing BMDM
383 phagolysosomes and the established bet-hedging strategy of host macrophages in silico. We found that
384 if a *C. neoformans* yeast were to trigger Dragotcytosis even just a single time if their original
385 phagolysosome dropped to pH < 4, it would be enough to drop the proportion of inhibitory phagosomes
386 from ~15% to ~1% (**Figure 3C and D**). The actual effect on *C. neoformans* survival would be even more
387 pronounced since Dragotcytosis events are not limited to one event per yeast in vitro/vivo. We then
388 investigated how beneficial Dragotcytosis would be at a range of pH cutoffs, assuming that an ingested
389 *C. neoformans* would be equally likely to migrate into an M0, M1, or M2 macrophage. In the context of
390 pH, the benefit of a Dragotcytosis event increases steadily the further away from an optimal pH the
391 original phagolysosome is (**Figure 3E**).

392

393 *Cryptococcus neoformans* Does not Display an Inherent Bias for Destination Macrophages

394 While there is no obvious and apparent method for *C. neoformans* to specifically target M2
395 macrophages as the Dragotcytosis destination, such a system could still be possible. The donor and
396 acceptor macrophages maintain physical contact during the Dragotcytosis process, and an immune
397 synapse could transduce signals detectable by the ingested yeast. To investigate whether *C. neoformans*
398 shows a preference during Dragotcytosis we compared the rates of transfer from infected M1
399 macrophages to uninfected M1 or M2 macrophages. If there is a preference, then we would expect to
400 observe an increased amount of *C. neoformans* residing in M2 macrophages 24 HPI; if there were no
401 preference, we would expect to see equal transfer into M1 and M2 macrophages. Instead, we see
402 roughly an equivalent amount of transfer into M1 and M2 macrophages with slightly less transfer into
403 M0 macrophages (**Figure 4A and B**). Based on a model of Dragotcytosis dynamics, we expect it would
404 take approximately 4 to 5 sequential transfer events before we would be able to detect differences in
405 population based on random chance alone (**Figure 4C**).

406

407 *Proposed Model for Triggering Dragotcytosis*

408 Dragotcytosis requires live *C. neoformans* and its frequency is modulated by variables that effect stress
409 on the fungal cell (Supplemental Table 1). We synthesize these observations into a model whereby
410 stress in the phagolysosome, resulting in fungal cell damage, triggers a program for exiting the host cell.
411 We know that exocytosis is associated with actin flashes^{7,26} and posit that stressed cells activate a
412 program that manipulates the host cell to promote a choreography of events resulting in transit from
413 the phagolysosome to outside of the host cell (Figure 5). If these events lead to exocytosis at the cell
414 membrane region in contact with an adjoining macrophage, then non-lytic exocytosis becomes
415 Dragotcytosis. Given that non-lytic exocytosis has been observed in mammalian, fish, insect, and
416 protozoal cells the exit program is likely to target conserved functions in eukaryotic phagocytic cells^{6,8,27-}
417 ²⁹. As to whether apposition of two macrophages induces changes in the infected cell that are sensed by
418 the fungal cell is unknown and a subject for future investigation.

419

420 Discussion

421 Dragotcytosis is a cellular process by which *C. neoformans* yeasts within a host macrophage
422 phagolysosome transfer to another, proximal macrophage without lysis of the initial host^{6,8,9,11}. During
423 recent investigations into the receptors used in Dragotcytosis and into the phagolysosomal acidification
424 dynamics of macrophages, we found a correlation between phagolysosomal hospitality and the
425 frequency of Dragotcytosis and suggesting that Dragotcytosis is beneficial to, and triggered by, ingested
426 *C. neoformans*^{9,10}. This led us to hypothesize that fungal discomfort in the phagosome was a trigger for
427 cell-to-cell transfer and in this study, we demonstrate that cellular stress on *C. neoformans* leads to
428 increased Dragotcytosis frequency.

429

430 Previous studies have shown that M2 macrophages and Th2 skewed immune responses are more
431 permissive to *C. neoformans* infection³⁰⁻³³. Our initial observation that M2 macrophages have, on
432 average, higher pH phagolysosomes compared to M1 macrophages when containing inert particles
433 offers a partial explanation of why these macrophages are more hospitable. Specifically, M2
434 macrophage populations had the fewest phagolysosomes at an inhibitory pH (pH < 4) and the most
435 phagolysosomes in an optimal pH range (5 < pH < 6) for fungal growth²⁰. Additionally, we noticed that *C.*
436 *neoformans* underwent fewer Dragotcytosis events when residing in M2 macrophage phagolysosomes
437 compared to yeast cells resident in M1 macrophages. From this correlation, we hypothesized that if the
438 phagolysosomal pH dropped too low for an ingested *C. neoformans* to counter with its polysaccharide
439 capsule or urease activity^{3,5,34,35}, then it triggered either non-lytic exocytosis or Dragotcytosis as an
440 escape mechanism that would bring the yeast cell to the less acidic extracellular environment or into a
441 phagolysosome of more hospitable pH, respectively.

442

443 Since phagolysosomal pH is stochastically determined with a distribution in which most phagosomes
444 have pH > 4, it is likely that *C. neoformans* residing in a phagosome with pH < 4 would find a more
445 hospitable home after a Dragotcytosis event¹⁰. Consequently, we probed how Dragotcytosis could
446 modulate the effectiveness of the macrophage acidification bet hedging strategy via in silico modeling
447 and found that even a single Dragotcytosis event triggered for *C. neoformans* residing in low pH
448 phagolysosomes would significantly increase the likelihood of finding a less acidic phagosome. These
449 findings could also help explain how *C. neoformans* replicates faster inside macrophages *in vivo* and *in*
450 *vitro* than in the extracellular space, which has been attributed to faster replication in the acidic pH of
451 the average phagosome³⁶⁻³⁸. Despite not all phagosomes being conducive to faster fungal growth,
452 sequential Dragotcytosis events could lead *C. neoformans* to find phagolysosomes more permissive to
453 rapid growth during an infection. These results fit well with the known data of *C. neoformans* infection
454 in human macrophages. Human macrophage phagolysosomes acidify with different dynamics than
455 those of mice. For example, human M2 macrophage phagolysosomes acidify to a lower pH than mouse
456 macrophage phagolysosomes³⁹ and, perhaps as a result, humans are markedly resistant to *C.*
457 *neoformans* infection which poses little threat to most immune competent hosts. Additionally, human
458 macrophages undergo both Vomocytosis and Dragotcytosis with much greater frequency than mouse
459 macrophages *in vitro*, consistent with the hypothesis that both processes are triggered by fungal
460 residence in hostile phagolysosomes.

461

462 To probe deeper into whether there was a causal association between average phagolysosomal pH of
463 M1 macrophages and the frequency of Dragotcytosis, we treated macrophages with either chloroquine
464 or bafilomycin A1, keeping phagolysosomal pH near the optimal growth range of *C. neoformans* and
465 comparable to the observed average phagolysosomal pH of M2 macrophage populations. We found that
466 both chloroquine and bafilomycin A1 drastically reduced Dragotcytosis events, supporting the
467 hypothesis that cellular stress is the stimulus for Dragotcytosis. We are confident that the drug
468 treatments themselves did not have a direct effect on *C. neoformans* growth, virulence, or survivability
469 at the concentrations used but rather modulated the host macrophage response. Chloroquine does not
470 significantly reduce *C. neoformans* growth or viability unless ingested by macrophages and at
471 concentrations higher than used in these experiments⁴⁰. Similarly, at high concentrations Bafilomycin A1
472 has antifungal⁴¹ and even inhibits *C. neoformans* melanization⁴² but the concentrations used here are
473 much lower than those associated with antifungal effects⁴³. We also treated cells with sub-inhibitory
474 concentrations of fluconazole and amphotericin B, to explore whether these drugs would also stress the
475 yeast in a way that promotes Dragotcytosis⁴⁴. Interestingly, both antifungal drugs reduced the overall
476 frequency of Dragotcytosis possibly because the concentrations were still too disruptive to fungal
477 metabolism and the yeast was too compromised to transfer. In this regard, both drugs affect fungal
478 membrane ergosterol integrity and fungal lipids may be required for the Dragotcytosis process.
479 Alternatively, ergosterol disruption is not sensed by the fungal machinery that triggers Dragotcytosis.

480

481 To further investigate the oxidative trigger hypothesis, we characterized Dragotcytosis frequencies of
482 several *C. neoformans* strain KN99 mutants from a knockout library during infection. We selected a
483 variety of potential candidates based on known pathways relevant to our cellular stress hypothesis. We
484 found that SOD1, Cat1, Cat3, TXN, GPx, and GPx2 deficient mutants underwent Dragotcytosis drastically
485 more frequently than the wild-type parental strain, supporting the notion that Dragotcytosis is triggered
486 by the accumulation of oxidative stress. Interestingly, knocking out SOD2 and TXN2 did not increase
487 frequency of Dragotcytosis which may reflect the nature of the phagolysosomal oxidative stress, as
488 SOD1 and SOD2 are known to have different efficacy against different oxidative stresses⁴⁵.

489

490 If oxidative stress triggers Dragotcytosis, then reducing stress within the phagolysosome should reduce
491 the frequency of Dragotcytosis. Melanin is known to protect *C. neoformans* from oxidative stress⁴⁶.
492 Melanized *C. neoformans* triggered Dragotcytosis at a lower frequency compared to non-melanized *C.*
493 *neoformans*. The cryptococcal capsule is known to protect against both pH and ROS in macrophages.
494 Macrophages infected with *C. neoformans* with large capsules manifested Dragotcytosis at a reduced
495 rate, though Vomocytosis occurred at an increased rate. It is less clear whether Vomocytosis is triggered
496 by the yeast or host as heat killed *C. neoformans* have been observed to undergo Vomocytosis, albeit at
497 a drastically reduced rate⁷, raising the question of what could trigger one pathway opposed to the other.
498 When macrophage infection was done at a temperature optimal for *C. neoformans* and suboptimal for
499 macrophages: 30 °C we again found that Dragotcytosis frequency was reduced.

500

501 We next considered whether *C. neoformans* induced a bias toward M2 macrophages as acceptor
502 macrophages in the Dragotcytosis process. Logically it would benefit the yeast as M2 macrophages were
503 found to be more permissive, but a mechanism by which the yeast could sense interaction with an M2
504 macrophage and initiate the Dragotcytosis process all from within the phagolysosome is difficult to
505 imagine. Thus, we designed an experiment in which infected M1 macrophages would be seeded with
506 labelled and uninfected M1 or M2 macrophages and we would compare the rate of transfer. If there
507 was a preference, we should see an unequal rate of transfer between the two populations. Instead, we
508 observed equal rates of transfer into both macrophage types. We expect that, given enough time, the
509 distribution would shift to favor M2 macrophages by random chance. However, this was not observed
510 due to the infrequency of sequential macrophage-to-macrophage transfers by a single cryptococcal cell
511 during the first 24 hours of experimental observation. Thus, we find it more likely that *C. neoformans*
512 initiates a transfer without prior knowledge of the receiver macrophage and instead would continue
513 transferring until a hospitable phagolysosome is discovered by chance.

514

515 Dragotcytosis was stochastically initiated, reflecting the dynamics of phagolysosome acidification¹⁰.
516 However, unlike phagosomal acidification, which manifested a normal distribution, the distribution of
517 Dragotcytosis as a function of time was skewed away from normality. Therefore, while phagolysosomal
518 pH contributes to triggering Dragotcytosis, it is likely not the only important trigger, a hypothesis
519 supported by previous observations that inhibiting pH buffering via urease mutation did not increase
520 Dragotcytosis events as would be expected if the process was triggered by pH alone⁵. Instead,
521 Dragotcytosis may be triggered by an accumulation of diverse sources of cellular stress encountered in
522 the phagolysosome. Whereas the endpoint of phagolysosomal acidification represents a bet hedging
523 strategy by macrophages to control ingested microbes¹⁰, *C. neoformans* also appears to be employing a
524 bet hedging strategy in exocytosis that is triggered by the bet-hedging strategy in macrophage
525 phagolysosome acidification. In fact, *C. neoformans* may engage in its own bet hedging strategy wherein
526 Dragotcytosis is triggered past a certain threshold of stress in which it becomes more likely that the
527 ingested yeast will migrate to a more hospitable phagolysosome. This results in the interesting situation
528 whereby a defensive strategy by the host cells is co-opted for survival by the fungal cell. Hence, chance
529 outcomes in the phagolysosome trigger events that produce chance outcomes in macrophage
530 exocytosis, implying connectivity between these two cellular processes with regards to their system
531 dynamics. Stochastic processes are random and thus inherently unpredictable, suggesting a
532 fundamental unpredictability to cellular processes that could extend to making host-microbe
533 interactions not predictable.

534

535 In summary, our results consistently show that conditions that increase or decrease *C. neoformans*
536 oxidative stress are associated with enhanced and reduced Dragotcytosis, respectively. However, it may
537 be impossible to narrow down Dragotcytosis triggers to one specific stressor. The drugs that inhibit
538 phagosome acidification can also inhibit autophagy, and vice versa, making it difficult to parse out the
539 effects of only one of these systems at a time. Even the generation of reactive oxygen species is innately
540 tied to these processes, and phagolysosomal pH itself, with the concentration of ROS in the
541 phagolysosome increasing alongside pH with previously measured concentrations of 50 μM $\text{O}_2^{\bullet-}$ at pH
542 7.4 and 2 μM at pH 4.5¹³. We find it more likely that a combination of cellular stresses triggers

543 Dragotcytosis and our findings suggest that initiation of Dragotcytosis is a downstream product of
544 overwhelming stress in the phagolysosome. We note how the normally distributed phagolysosomal pH
545 following phagocytosis randomly includes some phagolysosomes that are inhospitable to fungal cells
546 which, in turn, triggers exocytosis with its own stochastic dynamics with a unique distribution, as other
547 factors contribute to the exit phenomenon. Hence, stochastic dynamics in phagosomal acidification
548 beget stochastic dynamics in non-lytic exocytosis, implying a fundamentally unpredictable host-microbe
549 interaction at the level of cellular organelles. Such unpredictability at the cellular level is a likely
550 contributor to our inability to predict the outcome of host-microbe interactions at the organismal
551 level⁴⁷.

552

553 Acknowledgements

554 This work was funded in part by NIH grant 5R01HL059842-21.

555

556 References

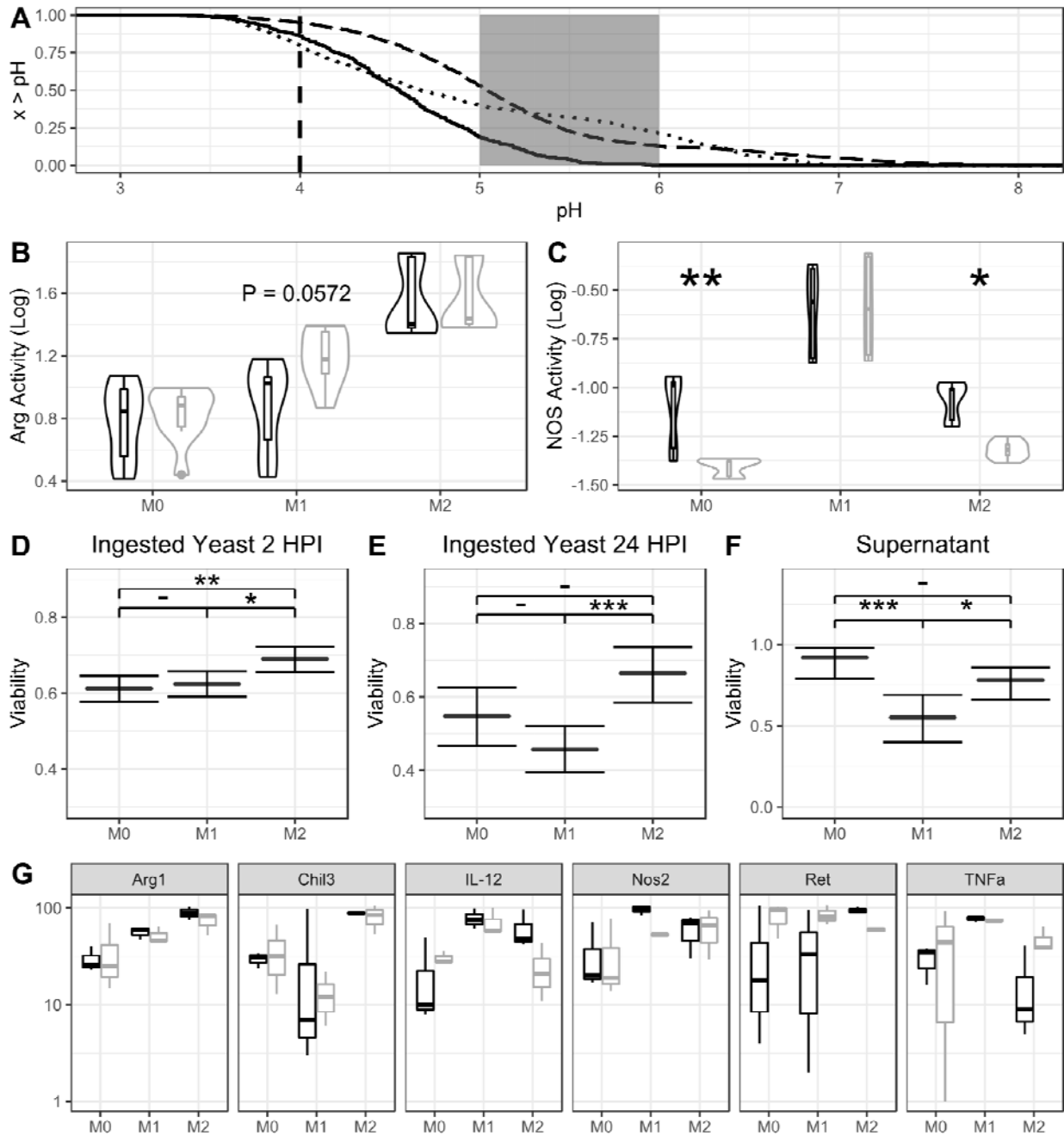
- 557 1. Levitz, S. M.; Nong, S. H.; Seetoo, K. F.; Harrison, T. S.; Speizer, R. A.; Simons, E. R. *Cryptococcus*
558 *neoformans* resides in an acidic phagolysosome of human macrophages. *Infection and Immunity*
559 **67**, 885–890 (1999).
- 560 2. Bojarczuk, A.; Miller, K. A.; Hotham, R.; Lewis, A.; Ogryzko, N. V.; Kamuyango, A. A.; Frost, H.;
561 Gibson, R. H.; Stillman, E.; May, R. C.; Renshaw, S. A.; Johnston, S. A. *Cryptococcus neoformans*
562 Intracellular Proliferation and Capsule Size Determines Early Macrophage Control of Infection.
563 *Scientific Reports* **6**, 21489 (2016). [PMID:26887656]
- 564 3. De Leon-Rodriguez, C. M.; Fu, M. S.; Corbali, M. O.; Cordero, R. J. B.; Casadevall, A. The Capsule of
565 *Cryptococcus neoformans* Modulates Phagosomal pH through Its Acid-Base Properties. *mSphere*
566 **3**, (2018). [PMID:30355667]
- 567 4. Smith, L. M.; Dixon, E. F.; May, R. C. The fungal pathogen *Cryptococcus neoformans* manipulates
568 macrophage phagosome maturation. *Cellular Microbiology* **17**, 702–713 (2015).
569 [PMID:25394938]
- 570 5. Fu, M. S.; Coelho, C.; De Leon-Rodriguez, C. M.; Rossi, D. C. P.; Camacho, E.; Jung, E. H.; Kulkarni,
571 M.; Casadevall, A. *Cryptococcus neoformans* urease affects the outcome of intracellular
572 pathogenesis by modulating phagolysosomal pH. *PLOS Pathogens* **14**, e1007144 (2018).
- 573 6. Alvarez, M.; Casadevall, A. Cell-to-cell spread and massive vacuole formation after *Cryptococcus*
574 *neoformans* infection of murine macrophages. *BMC immunology* **8**, 16 (2007).
- 575 7. Alvarez, M.; Casadevall, A. Phagosome Extrusion and Host-Cell Survival after *Cryptococcus*
576 *neoformans* Phagocytosis by Macrophages. *Current Biology* **16**, 2161–2165 (2006).
- 577 8. Ma, H.; Croudace, J. E.; Lammas, D. A.; May, R. C. Direct cell-to-cell spread of a pathogenic yeast.
578 *BMC immunology* **8**, 15 (2007). [PMID:17705831]
- 579 9. Dragotakes, Q.; Fu, M. S.; Casadevall, A. Dragotcytosis: Elucidation of the Mechanism for
580 *Cryptococcus neoformans* Macrophage-to-Macrophage Transfer. *The Journal of Immunology*

- 581 ji1801118 (2019). [PMID:30877168]
- 582 **10.** Dragotakes, Q.; Stouffer, K. M.; Fu, M. S.; Sella, Y.; Youn, C.; Yoon, O. I.; De Leon-Rodriguez, C. M.;
583 Freij, J. B.; Bergman, A.; Casadevall, A. Macrophages use a bet-hedging strategy for antimicrobial
584 activity in phagolysosomal acidification. *The Journal of clinical investigation* **130**, 3805–3819
585 (2020). [PMID:32298242]
- 586 **11.** Ma, H.; Croudace, J. E.; Lammas, D. A.; May, R. C. Expulsion of Live Pathogenic Yeast by
587 Macrophages. *Current Biology* **16**, 2156–2160 (2006). [PMID:17084701]
- 588 **12.** Nicola, A. M.; Robertson, E. J.; Albuquerque, P.; Derengowski, L. da S.; Casadevall, A. Nonlytic
589 Exocytosis of *Cryptococcus neoformans* from Macrophages Occurs In Vivo and Is Influenced by
590 Phagosomal pH. *mBio* **2**, e00167-11 (2011). [PMID:21828219]
- 591 **13.** Slauch, J. M. How does the oxidative burst of macrophages kill bacteria? Still an open question.
592 *Molecular Microbiology* **80**, 580–583 (2011).
- 593 **14.** Nguyen, G. T.; Green, E. R.; Meccas, J. *Frontiers in Cellular and Infection Microbiology*. Frontiers
594 Media S.A. August 25, 2017
- 595 **15.** Nordenfelt, P.; Tapper, H. Phagosome dynamics during phagocytosis by neutrophils. *Journal of*
596 *Leukocyte Biology* **90**, 271–284 (2011). [PMID:21504950]
- 597 **16.** Voelz, K.; Johnston, S. A.; Rutherford, J. C.; May, R. C. Automated analysis of cryptococcal
598 macrophage parasitism using GFP-tagged cryptococci. *PLoS. ONE* **5**, e15968 (2010).
- 599 **17.** Liu, O. W.; Chun, C. D.; Chow, E. D.; Chen, C.; Madhani, H. D.; Noble, S. M. Systematic Genetic
600 Analysis of Virulence in the Human Fungal Pathogen *Cryptococcus neoformans*. *Cell* **135**, 174–
601 188 (2008).
- 602 **18.** Dragotakes, Q.; Casadevall, A. Automated measurement of cryptococcal species polysaccharide
603 capsule and cell body. *Journal of Visualized Experiments* **2018**, (2018).
- 604 **19.** Zunino, L.; Soriano, M. C.; Rosso, O. A. Distinguishing chaotic and stochastic dynamics from time
605 series by using a multiscale symbolic approach. *Phys. Rev. E. Stat. Nonlin. Soft. Matter Phys* **86**,
606 46210 (2012).
- 607 **20.** De Leon-Rodriguez, C. M.; Rossi, D. C. P.; Fu, M. S.; Dragotakes, Q.; Coelho, C.; Guerrero Ros, I.;
608 Caballero, B.; Nolan, S. J.; Casadevall, A. The Outcome of the *Cryptococcus neoformans*–
609 Macrophage Interaction Depends on Phagolysosomal Membrane Integrity. *The Journal of*
610 *Immunology* **201**, 583–603 (2018).
- 611 **21.** Weinberg, P. B.; Becker, S.; Granger, D. L.; Koren, H. S. Growth inhibition of *Cryptococcus*
612 *neoformans* by human alveolar macrophages. *Am. Rev. Resp. Dis* **136**, 1242–1247 (1987).
- 613 **22.** Granger, D. L.; Perfect, J. R.; Durack, D. T. Macrophage-mediated fungistasis in vitro: requirements
614 for intracellular and extracellular cytotoxicity. *J. Immunol* **136**, 672–680 (1986).
- 615 **23.** Jacobson, E. S.; Hove, E.; Emery, H. S. Antioxidant function of melanin in black fungi. *Infect.*
616 *Immun* **63**, 4944–4945 (1995).
- 617 **24.** Bustamante, J.; Bredeston, L.; Malanga, G.; Mordoh, J. Role of melanin as a scavenger of active
618 oxygen species. *Pigment Cell Res* **6**, 348–353 (1993).

- 619 **25.** Nosanchuk, J. D.; Casadevall, A. The contribution of melanin to microbial pathogenesis. *Cell*
620 *Microbiol* **5**, 203–223 (2003).
- 621 **26.** Johnston, S. A.; May, R. C. The human fungal pathogen *Cryptococcus neoformans* escapes
622 macrophages by a phagosome emptying mechanism that is inhibited by Arp2/3 complex-
623 mediated actin polymerisation. *PLoS Pathog* **6**, e1001041 (2010).
- 624 **27.** Davis, J. M.; Huang, M.; Botts, M. R.; Hull, C. M.; Huttenlocher, A. A Zebrafish Model of
625 Cryptococcal Infection Reveals Roles for Macrophages, Endothelial Cells, and Neutrophils in the
626 Establishment and Control of Sustained Fungemia. *Infection and Immunity* **84**, 3047–3062 (2016).
- 627 **28.** Qin, Q.-M.; Luo, J.; Lin, X.; Pei, J.; Li, L.; Ficht, T. A.; de Figueiredo, P. Functional analysis of host
628 factors that mediate the intracellular lifestyle of *Cryptococcus neoformans*. *PLoS pathogens* **7**,
629 e1002078 (2011).
- 630 **29.** Chrisman, C. J.; Alvarez, M.; Casadevall, A. Phagocytosis of *Cryptococcus neoformans* by, and
631 Nonlytic Exocytosis from, *Acanthamoeba castellanii*. *Applied and Environmental Microbiology* **76**,
632 6056–6062 (2010). [PMID:20675457]
- 633 **30.** Hoag, K. A.; Lipscomb, M. F.; Izzo, A. A.; Street, N. E. IL-12 and IFN-gamma are required for
634 initiating the protective Th1 response to pulmonary cryptococcosis in resistant C.B-17 mice. *Am.*
635 *J. Respir. Cell. Mol. Biol* **17**, 733–739 (1997).
- 636 **31.** Chen, G.-H.; McDonald, R. A.; Wells, J. C.; Huffnagle, G. B.; Lukacs, N. W.; Toews, G. B. The
637 Gamma Interferon Receptor Is Required for the Protective Pulmonary Inflammatory Response to
638 *Cryptococcus neoformans*. *Infection and Immunity* **73**, 1788–1796 (2005). [PMID:15731080]
- 639 **32.** Decken, K.; Kohler, G.; Palmer-Lehmann, K.; Wunderlin, A.; Mattner, F.; Magram, J.; Gately, M. K.;
640 Alber, G. Interleukin-12 is essential for a protective Th1 response in mice infected with
641 *Cryptococcus neoformans*. *Infect. Immun* **66**, 4994–5000 (1998).
- 642 **33.** Osterholzer, J. J.; Surana, R.; Milam, J. E.; Montano, G. T.; Chen, G.-H. H.; Sonstein, J.; Curtis, J. L.;
643 Huffnagle, G. B.; Toews, G. B.; Olszewski, M. A. Cryptococcal urease promotes the accumulation
644 of immature dendritic cells and a non-protective T2 immune response within the lung. *Am J*
645 *Pathol* **174**, 932–943 (2009). [PMID:19218345]
- 646 **34.** Cox, G. M.; Mukherjee, J.; Cole, G. T.; Casadevall, A.; Perfect, J. R. Urease as a virulence factor in
647 experimental cryptococcosis. *Infection and immunity* **68**, 443–448 (2000). [PMID:10639402]
- 648 **35.** Olszewski, M. A.; Noverr, M. C.; Chen, G. H.; Toews, G. B.; Cox, G. M.; Perfect, J. R.; Huffnagle, G.
649 B. Urease expression by *Cryptococcus neoformans* promotes microvascular sequestration,
650 thereby enhancing central nervous system invasion. *Am. J. Pathol* **164**, 1761–1771 (2004).
- 651 **36.** Feldmesser, M.; Kress, Y.; Novikoff, P.; Casadevall, A. *Cryptococcus neoformans* is a facultative
652 intracellular pathogen in murine pulmonary infection. *Infection and Immunity* **68**, 4225–4237
653 (2000).
- 654 **37.** Diamond, R. D.; Bennett, J. E. Growth of *Cryptococcus neoformans* within human macrophages in
655 vitro. *Infection and Immunity* **7**, 231–236 (1973). [PMID:4697791]
- 656 **38.** DeLeon-Rodriguez, C. M.; Casadevall, A. *Cryptococcus neoformans*: Tripping on Acid in the
657 Phagolysosome. *Frontiers in Microbiology* **7**, 164 (2016).

- 658 **39.** Canton, J.; Khezri, R.; Glogauer, M.; Grinstein, S. Contrasting phagosome pH regulation and
659 maturation in human M1 and M2 macrophages. *Molecular biology of the cell* **25**, 3330–3341
660 (2014). [PMID:25165138]
- 661 **40.** Levitz, S. M.; Harrison, T. S.; Tabuni, A.; Liu, X. Chloroquine induces human mononuclear
662 phagocytes to inhibit and kill *Cryptococcus neoformans* by a mechanism independent of iron
663 deprivation. *Journal of Clinical Investigation* **100**, 1640–1646 (1997).
- 664 **41.** WERNER, G.; HAGENMAIER, H.; DRAUTZ, H.; BAUMGARTNER, A.; ZÄHNER, H. Metabolic products
665 of microorganisms. 224. Bafilomycins, a new group of macrolide antibiotics. Production,
666 isolation, chemical structure and biological activity. *The Journal of Antibiotics* **37**, 110–117 (1984).
- 667 **42.** Erickson, T.; Liu, L.; Gueyikian, A.; Zhu, X.; Gibbons, J.; Williamson, P. R. Multiple virulence factors
668 of *Cryptococcus neoformans* are dependent on VPH1. *Molecular Microbiology* **42**, 1121–1131
669 (2001).
- 670 **43.** Harrison, T. S.; Griffin, G. E.; Levitz, S. M. Conditional lethality of the diprotic weak bases
671 chloroquine and quinacrine against *Cryptococcus neoformans*. *J. Infect. Dis* **182**, 283–289 (2000).
- 672 **44.** Nosanchuk, J. D.; Cleare, W.; Franzot, S. P.; Casadevall, A. Amphotericin B and fluconazole affect
673 cellular charge, macrophage phagocytosis, and cellular morphology of *Cryptococcus neoformans*
674 at subinhibitory concentrations. *Antimicrob. Agents Chemotherap* **43**, 233–239 (1999).
675 [PMID:9925511]
- 676 **45.** FrÄ©alle, E.; NoÄ«l, C.; Viscogliosi, E.; Camus, D.; Dei-Cas, E.; Delhaes, L. Manganese superoxide
677 dismutase in pathogenic fungi: An issue with pathophysiological and phylogenetic involvements.
678 *FEMS Immunology & Medical Microbiology* **45**, 411–422 (2005).
- 679 **46.** Wang, Y.; Aisen, P.; Casadevall, A. *Cryptococcus neoformans* melanin and virulence: mechanism
680 of action. *Infect. Immun* **63**, 3131–3136 (1995). [PMID:7622240]
- 681 **47.** Casadevall, A.; Pirofski, L. anne. What Is a Host? Attributes of Individual Susceptibility. *Infect*
682 *Immun* **86**, (2018). [PMID:29084893]
- 683

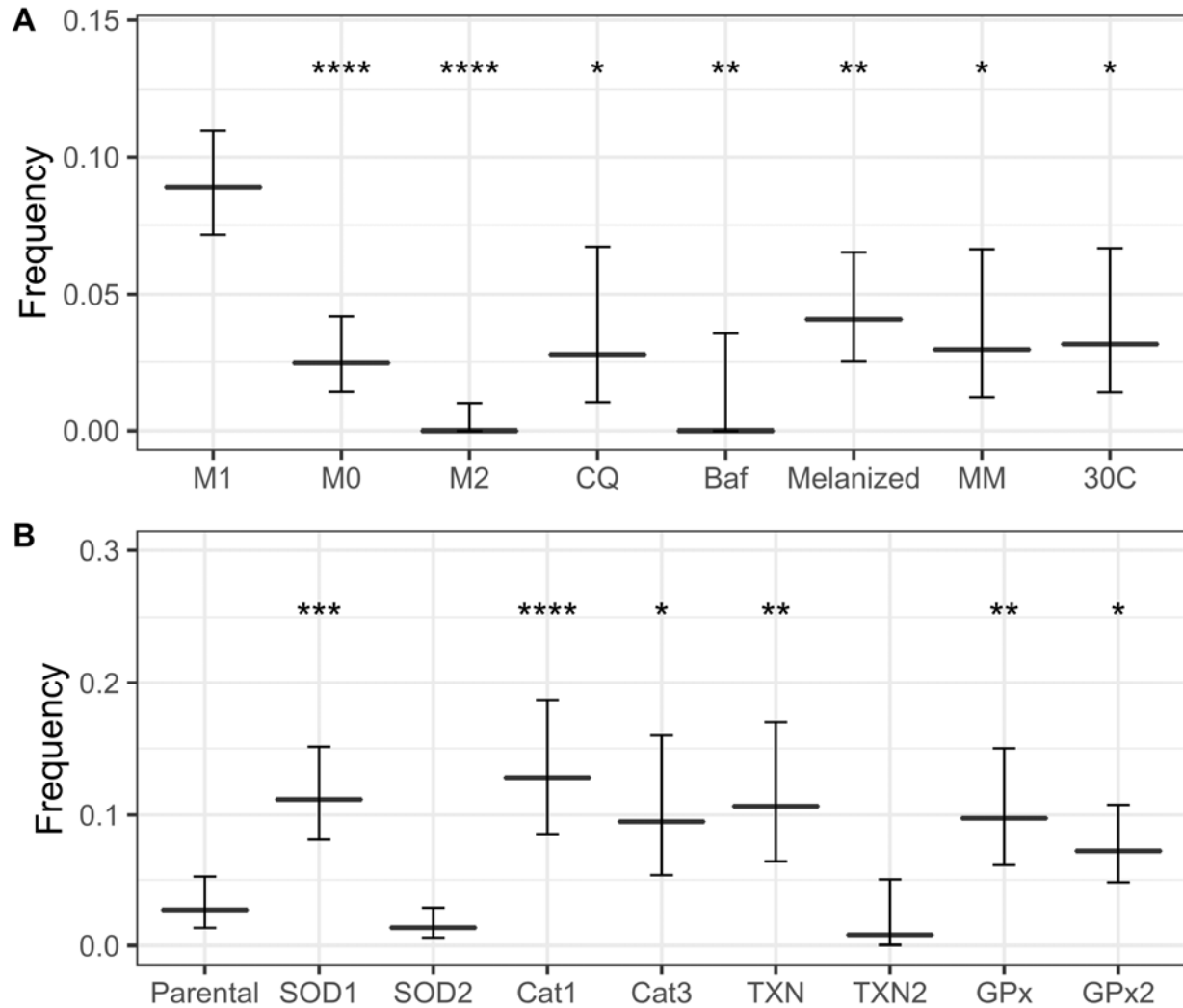
684 **Figures**



685

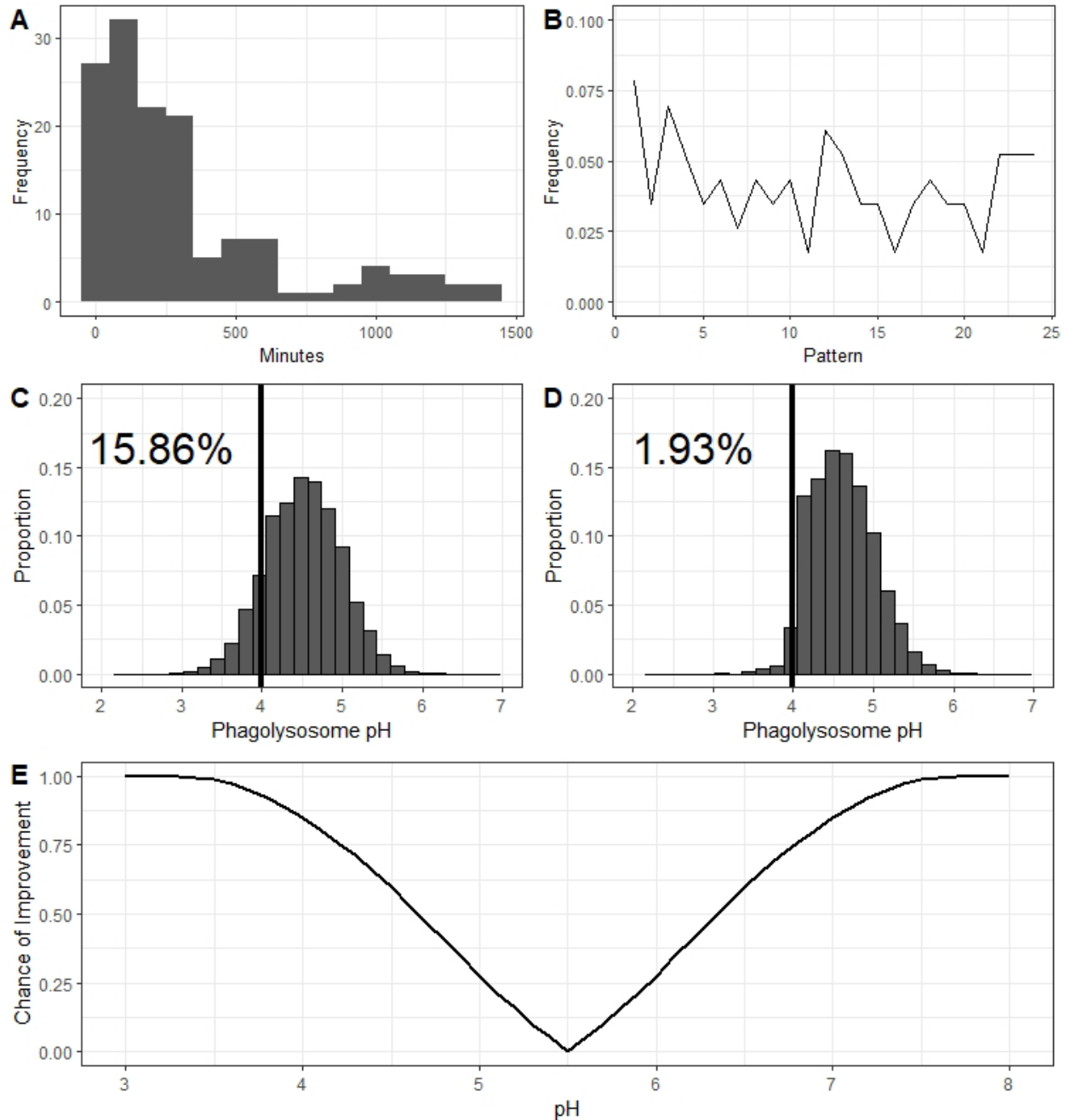
686 **Figure 1.** pH and Oxidative response in BMDM populations. **A.** Inverse empirical cumulative distribution
 687 functions for bead containing phagolysosome pH data measured in M0 (dotted), M1 (solid), and M2
 688 (dashed) macrophage populations. The dashed line at pH 4 represents the point at which pH inhibits *C.*
 689 *neoformans* replication while the gray area between pH 5 and 6 represents the optimal growth pH for *C.*
 690 *neoformans*. Hospitality of each population is estimated by the number of phagolysosomes within each
 691 of these regions. **B.** Arg-1 activity of differently polarized BMDMs infected (gray) or uninfected (black)
 692 with *C. neoformans*. M2 have the highest overall activity, and activity is promoted with infection in M1
 693 populations. **C.** NOS activity of differently polarized BMDMs infected (gray) or uninfected (black) with *C.*

694 *neoformans*. M1 have the highest overall activity, and activity is decreased with infection in both M0
695 and M2 populations. Significance determined by 2-way ANOVA with Tukey's HSD comparisons. **D.**
696 Viability of *C. neoformans* ingested by macrophage populations after 2 h. **E.** Viability of *C. neoformans*
697 ingested by macrophage populations after 2 h. **F.** Viability of extracellular *C. neoformans* after 24 h
698 incubation with macrophages. **G.** qPCR data from differently polarized BMDMs uninfected (black) and
699 infected (gray) with *C. neoformans* 24 HPI. Values are normalized to the respective M0 uninfected fold
700 induction. *, **, *** represent $P < 0.05$, 0.01, and 0.001, respectively. ANOVA with Tukey comparisons
701 were used in panels B and C while a test of equal proportions with Bonferroni correction was used in
702 panels D and E.



703

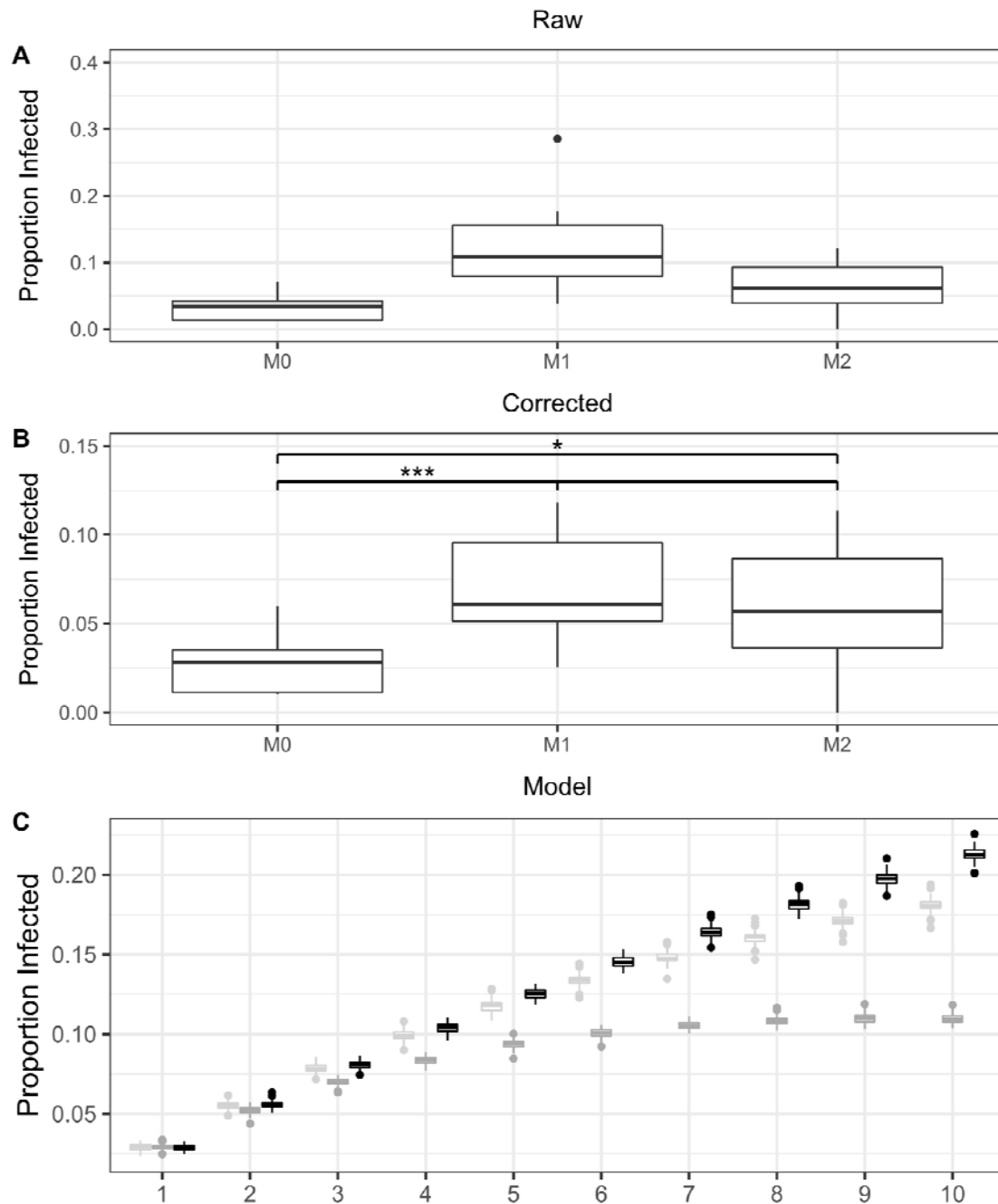
704 **Figure 2.** Dragotcytosis frequencies of *C. neoformans* ingested BMDMs under various conditions. **A.** *C.*
705 *neoformans* strain H99 frequencies of Dragotcytosis. M0 and M2 macrophages have lower frequencies
706 of Dragotcytosis overall compared to M1. Alkalizing the phagolysosomes of M1 macrophages with
707 chloroquine (Chloro) or bafilomycin A1 (BafA), protecting from ROS with melanin (Melanized),
708 stimulating capsule growth with minimal media conditions (MM), and inhibiting macrophage function
709 with low temperature (30C) also abrogate Dragotcytosis frequency. **B.** *C. neoformans* strain KN99α
710 Dragotcytosis frequencies among infected macrophages. Knocking out genes directly involved in
711 oxidative stress mitigation increases frequency of Dragotcytosis. Graphs depict means with 95%
712 confidence intervals. *, **, ***, **** denote $P < 0.05$, 0.01, 0.001, and 0.0001 via test of equal
713 proportions compared to M1 with Bonferroni correction for multiple hypotheses.



714

715 **Figure 3.** Dynamics of Dragotcytosis. **A.** Distribution of the times at which *C. neoformans* yeasts initiated
716 host cell exit strategies. Both Vomocytosis and Dragotcytosis events are represented here. Bin widths
717 are set to 100 and the data depicted spans 139 samples from 12 experiments. **B.** Ordinal pattern
718 analysis for the intervals between events. Intervals were gathered and analyzed within experiments and
719 total proportions of individual ordinal patterns summed between experiments. **C.** Hypothetical
720 phagolysosomal pH distributions if *C. neoformans* particles were to undergo no Dragotcytosis events. **D.**
721 Modelled phagolysosomal pH distributions if *C. neoformans* particles were to undergo one Dragotcytosis
722 event if their resident phagolysosomal pH is < 4. Even a single round of low pH triggered Dragotcytosis
723 drastically shifts the distribution to the right resulting in a greater proportion of *C. neoformans*
724 hospitable phagolysosomes. Labelled percent values reflect the proportion of hypothetical

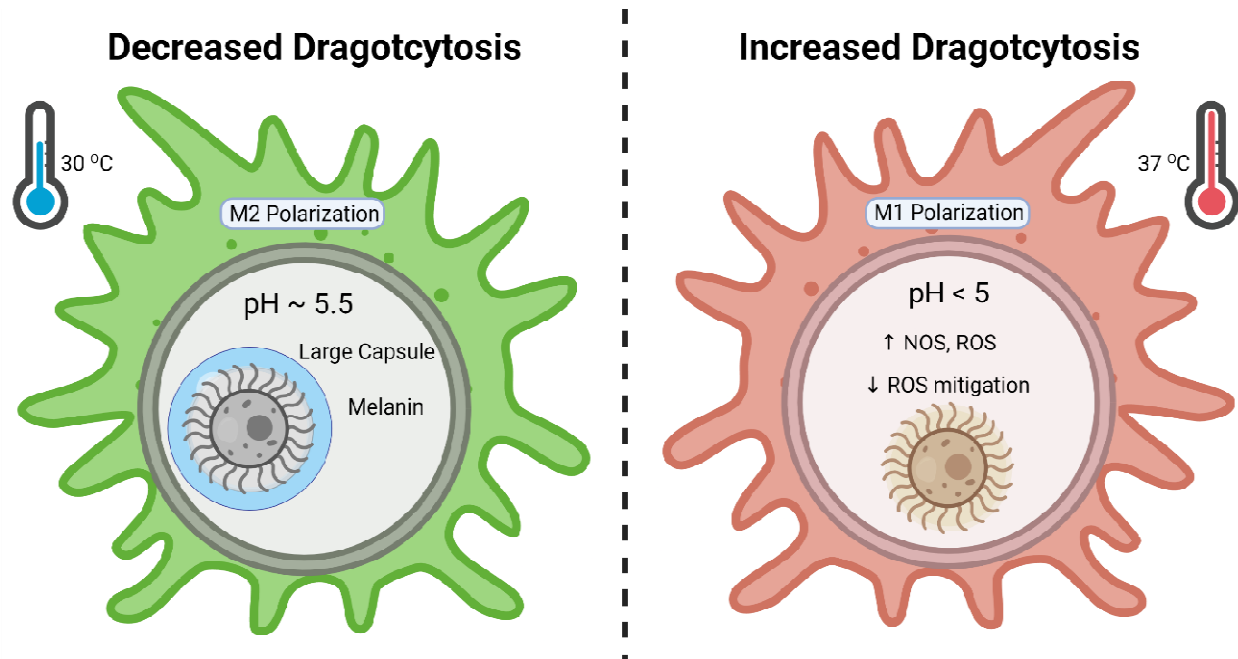
725 phagolysosomes inhibitory to *C. neoformans* (pH < 4, black vertical line) in each scenario. **E.** Hypothetical
726 chance of an ingested *C. neoformans* to find a more hospitable phagolysosome in the context of pH
727 assuming equal likelihood of migrating to an M0, M1, or M2 macrophage.



728

729 **Figure 4.** Comparisons of labelled macrophage populations and the proportion of which have ingested *C.*
730 *neoformans* 24 hours post infection. **A.** The uncorrected proportion of adherent macrophages
731 containing *C. neoformans* at the end of the infection. **B.** The proportion of macrophages containing
732 yeast after correcting for floating cells. Both the proportion of labelled cells compared to the original
733 population of infected M1 macrophages as well as the frequency of labelled cells which ingested *C.*
734 *neoformans* remained consistent throughout the time course. *, *** signify $P < 0.05$ and 0.001 via

735 ANOVA with Tukey multiple comparisons. C. A model depicting expected proportions of infected cells
736 based only on random chance after sequential Dragocytosis events for M0 (light gray), M1 (dark gray),
737 and M2 (black) macrophages.



738

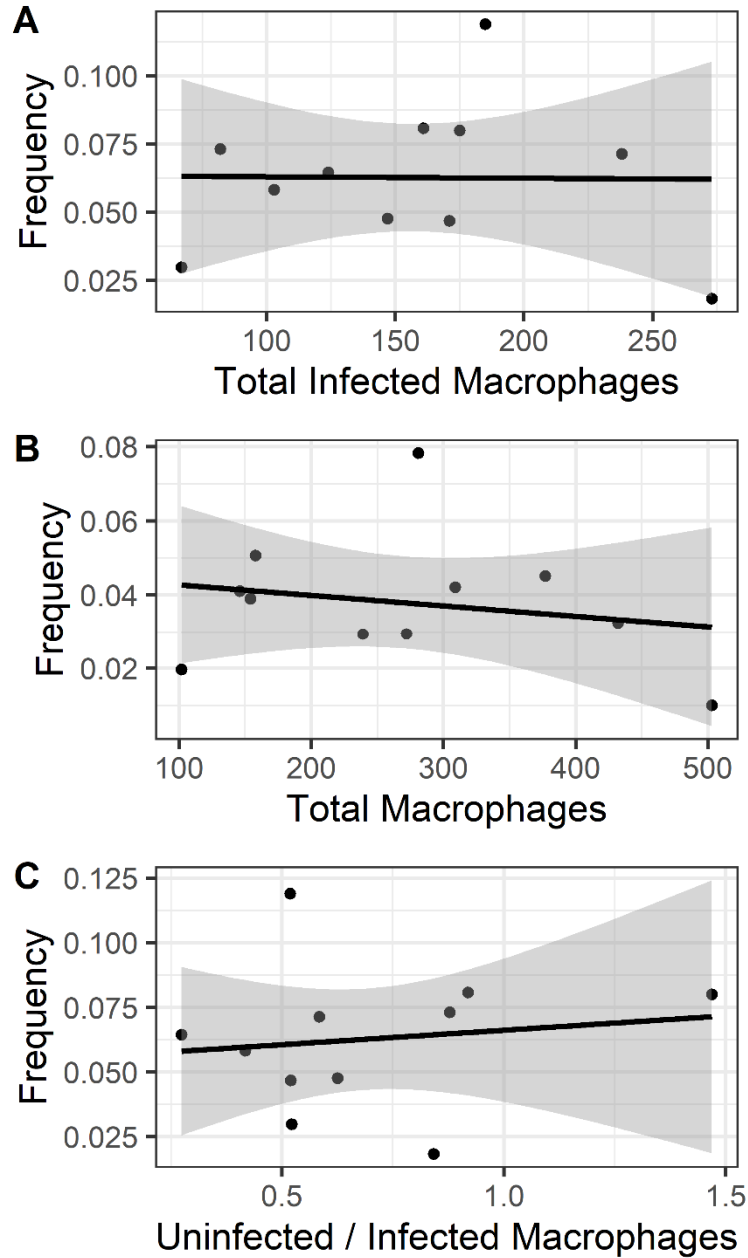
739 Figure 5

740 Graphical summary of conditions with effects on Dragotcytosis frequency. Figure was created with
741 BioRender.com.

742 Supplemental Table 1. Summary of variable effects on Dragotcytosis frequency.

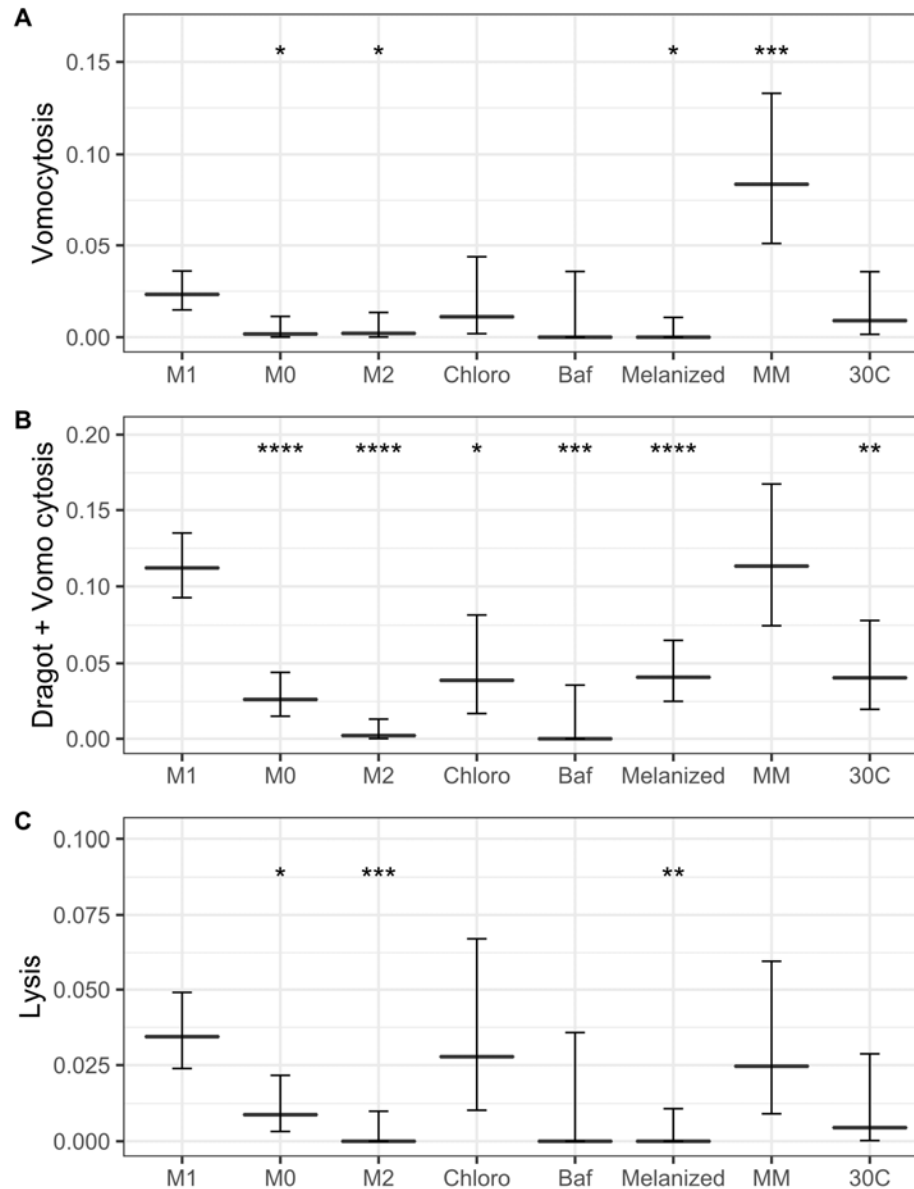
Frequency	Variable	Effect
Increase	Macrophage M1 Polarization	Enhanced antifungal activity (increased NO)
	Decreased Phagosome pH	Increased phagolysosome fungistatic mechanisms Reduced fungal growth
	CN Superoxide 1 Deficiency	Enhanced fungal susceptibility to oxidants
	CN Catalase 1 and 3 Deficiency	Enhanced fungal susceptibility to oxidants
	CN Thioredoxin Deficiency	Enhanced fungal susceptibility to oxidants
	CN Glutathione Peroxidase Deficiency	Enhanced fungal susceptibility to oxidants
Decrease	Macrophage M2 Polarization	Reduced antifungal activity
	Increased Phagosome pH	Reduced phagolysosome fungistatic mechanisms Enhanced fungal replication
	Bafilomycin A1 and Chloroquine Treatment	Increases phagolysosomal pH, reduced phagolysosome fungistatic mechanisms
	Fluconazole and Amphotericin B Treatment	Disrupts fungal ergosterol processes
	Melanin	Reduced fungal susceptibility to oxidants
	CN Urease Deficiency	Decreased phagosomal pH, increased intracellular CN replication, disrupted phagolysosomal membrane, increased apoptotic macrophages ⁵
	Increased Capsule Size	Increased buffering potential, reduced macrophage phagocytosis efficiency
	Temperature (30 °C)	Reduced macrophage function

743



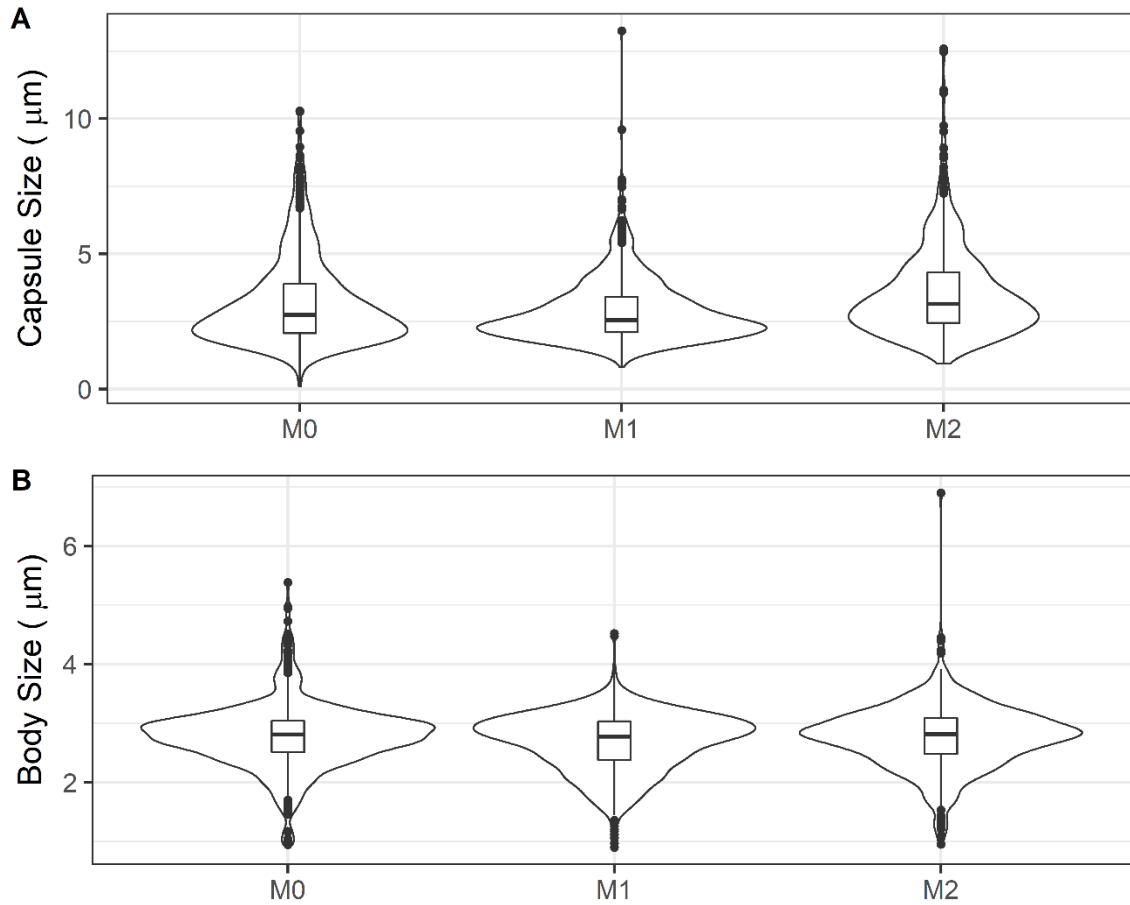
744

745 **Supplemental Figure 1.** Frequency of Dragotcytosis events of ingested *C. neoformans* H99 yeasts
746 according to population size of infected or total macrophages. **A.** Dragotcytosis frequency did not
747 correlate with total number of infected macrophages. **B.** Dragotcytosis frequency did not correlate with
748 the density of total macrophages. **C.** Dragotcytosis frequency did not correlate with the proportion of
749 uninfected to infected macrophages.



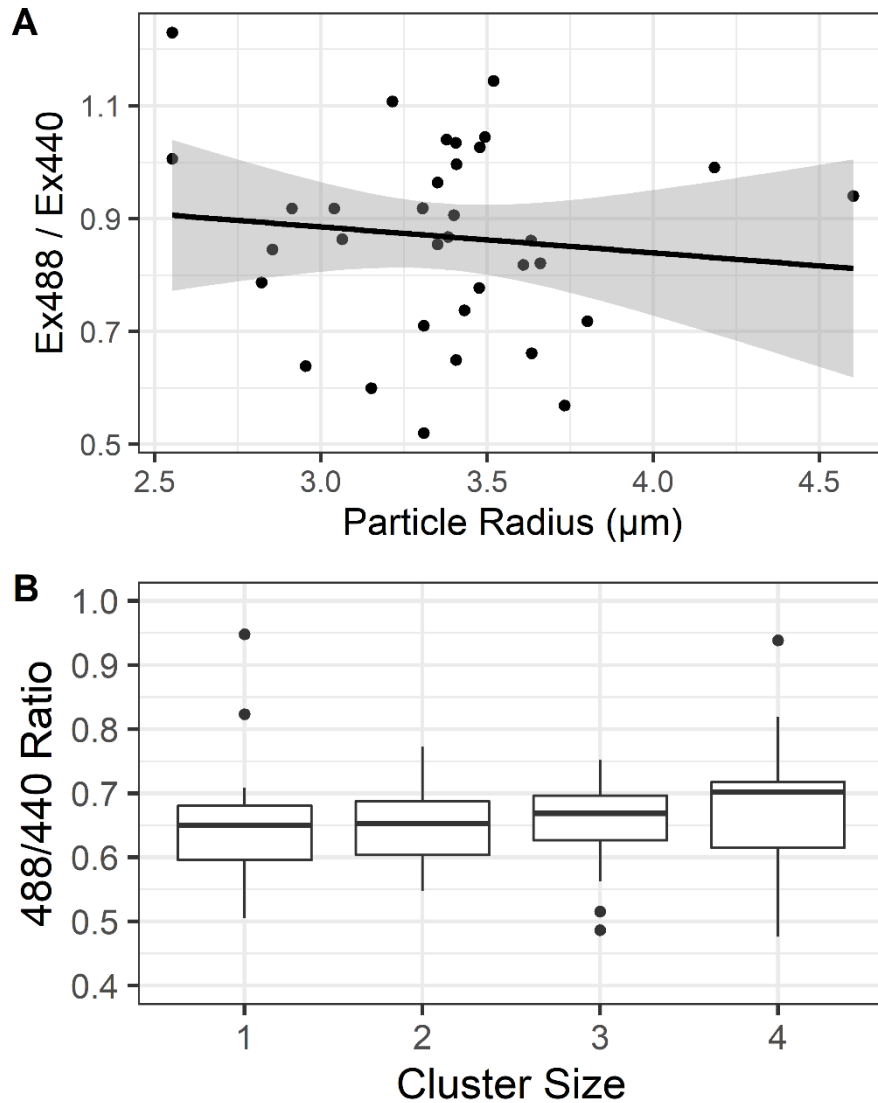
750

751 **Supplemental Figure 2.** Event frequencies of *C. neoformans* strain H99 ingested by BMDMs under
752 various pH related conditions. **A.** Vomocytosis frequency among infected macrophages. **B.** Combined
753 frequency of Dragotcytosis and Vomocytosis among infected macrophages. **C.** Lysis frequency among
754 infected macrophages. All conditions have similar frequency. Event frequencies of wild-type KN99 strain
755 and mutant *C. neoformans* after ingestion by M1 polarized BMDMs. *, **, ***, **** signify $P < 0.05$,
756 0.01, 0.001, and 0.0001 via test of equal proportions, respectively. Bonferroni correction was applied for
757 multiple hypotheses.



758

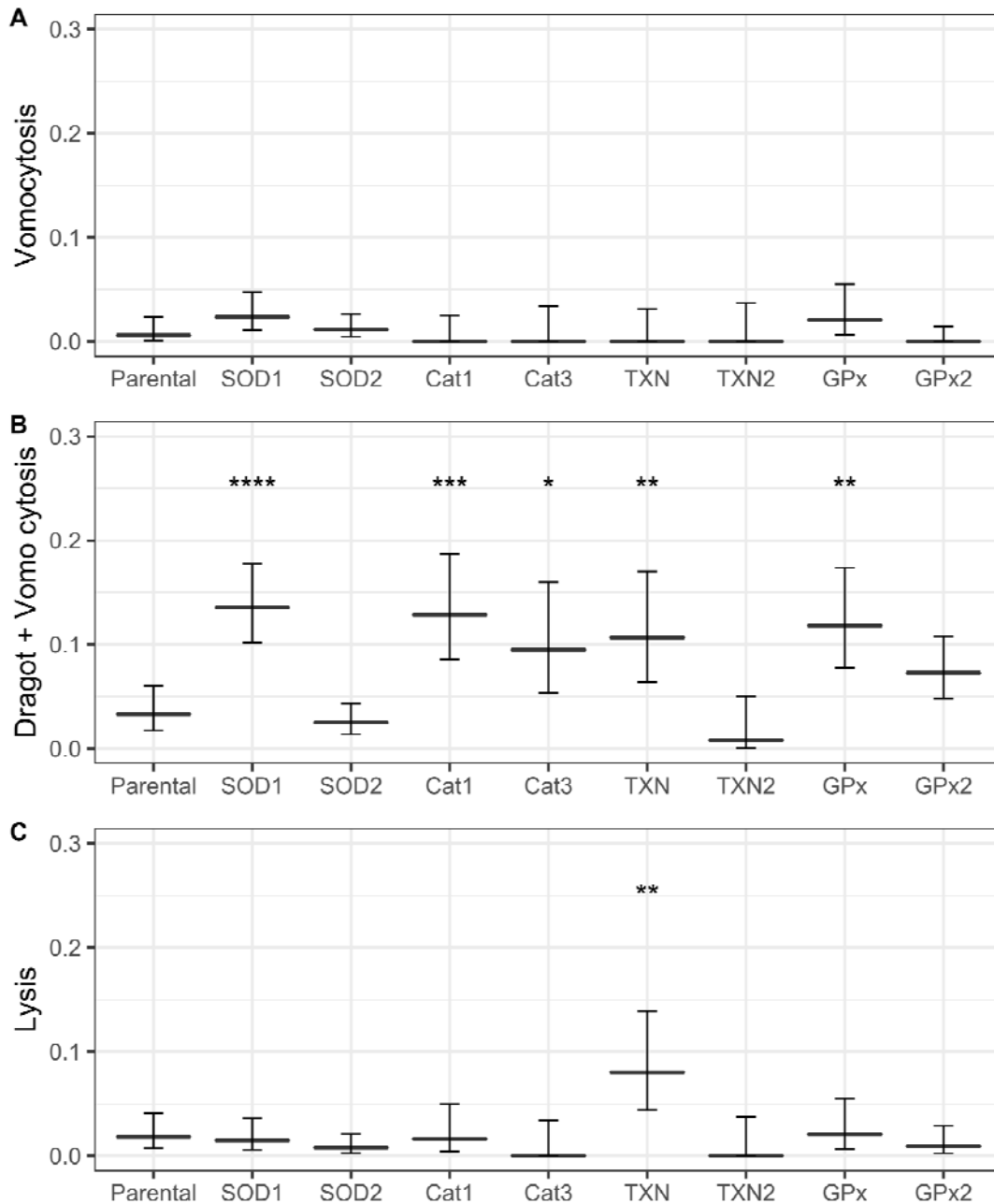
759 **Supplemental Figure 3.** Capsule and cell body size of *C. neoformans* isolated 24 hours after ingestion by
760 BMDMs. Capsules and cell bodies are measured by preparing and imaging India Ink slides and a
761 previously published¹⁸ measuring code. No significant differences were found between the polarization
762 states of host macrophages.



763

764 **Supplemental Figure 4.** Fluorescence ratio of ingested particles as a measurement of phagolysosomal
765 pH compared to total volume of ingested particles. **A.** Fluorescence ratio of ingested *C. neoformans*. We
766 found no significant correlation. **B.** Fluorescence ratio of ingested inert latex beads of 0.6 μm diameter.
767 Even with a cluster of four particles within a single phagosome we did not detect a threshold at which
768 size alone disrupts the phagolysosomal pH.

769



770

771 Supplemental Figure 5. Event frequencies of *C. neoformans* strain KN99 α and knockout mutants
772 ingested by M1 BMDMs. **A.** Vomocytosis frequency among infected macrophages **B.** Combined
773 Dragocytosis and Vomocytosis frequency among infected macrophages. **C.** Lysis frequency among
774 infected macrophages. Graphs depict means with 95% confidence intervals. *, **, ***, **** signify $P <$
775 0.05, 0.01, 0.001, and 0.0001 via test of equal proportions, respectively. Bonferroni correction was
776 applied for multiple hypotheses.